

EXPERIMENTAL EVIDENCE OF UNCERTAINTY IN SEISMIC RESPONSE OF MASONRY VAULTS

A. Baratta¹, I. Corbi¹, O. Corbi¹, D. Rinaldis²

¹ *Department of Structural Engineering, University of Naples "Federico II", Naples, Italy*

² *ENEA, Italian National Agency for New Technologies, Energy and Environment, Rome, Italy*

www.unina.it www.enea.it

ABSTRACT :

This paper is focused on the correlation between the experimental results and the theoretical results. The experimental part is relevant to dynamic experimental tests performed on some masonry arches placed on a shaking table facility at the Laboratory of the ENEA Research Center. The theoretical part consists of two elaborations, the first one sees the elaboration of a model NT of the masonry structure, by means of some calculus codes made by the researchers of the University of Naples "Federico II", in the second part the implementation of the calculus code and of the recorded data is developed for the comparison of the theoretical model and the experimental one. The analysis puts in evidence that the static degradation of the simulacra is much faster than in the seismic response, probably thanks to kinetic energy absorption that helps the structure to resist inertia forces.

KEYWORDS: Masonry vaults, seismic action, uncertainty, shaking table, experimental tests.

1. INTRODUCTION

The paper aims at investigating some features of uncertainty of seismic response of masonry vaults on the basis of a pretty wide experimental campaign developed at the Laboratory of the ENEA research centre of Casaccia in cooperation with the University of Naples "Federico II" e with the Supervision Authority of Monumental Heritage of Caserta and Benevento countries.

The study is devoted to emphasize the peculiar character of the seismic action, whose effects on masonry constructions are usually characterized by not always sharply foreseeable results, due to the behavior of masonry which exhibits some uncertainty in its dynamic response. This objective is pursued by the suitable development and elaboration of the experimental data obtained from testing masonry vaults prototypes characterized by the same mechanical and geometrical properties and materials which are subject to the same dynamic signals inferred as base accelerations with different peak accelerations by means of a dynamic mono-directional shaking table. On the basis of the response data deriving from the used test accelerograms, which reproduce recorded earthquakes scaled at progressively increasing intensities, one may figure out the difficulty in obtaining properly reliable results in terms of damage prediction by means of experimental and, especially, theoretical investigations.

Actually, the experimental evidence shows not negligible differences in the dynamic response of two prototypes of the nominally same masonry structure subject to the same seismic action; in more details, the first arcade, damaged by diffused cracks under the shake, does not reaches the crisis, even if the cracks are arranged in such a way to activate any kinetic mechanism; on the contrary the second prototype, even if built by following the same path as for the first model, exhibits a more limited skill of absorbing the incoming energy, approaching the collapse condition for a lower shake intensity. From laboratory observations, one can maybe recognize the first cause of this behavior in a local incremental damage phenomenon due to the flattening of the unilateral hinge at the keystone, which shows a low resistance in the second model, thus reducing the stability of the mechanism in the second case.

2. THE MASONRY ARCH MODELLED AS A NO-TENSION STRUCTURE

In structural patterns of the type of arches, the stress field can be inferred from the internal forces on every cross section (Baratta & Corbi, 2003; 2005). The set of stress fields in equilibrium with applied loads can be built up

by a superposition scheme of the type shown in Fig. 1.

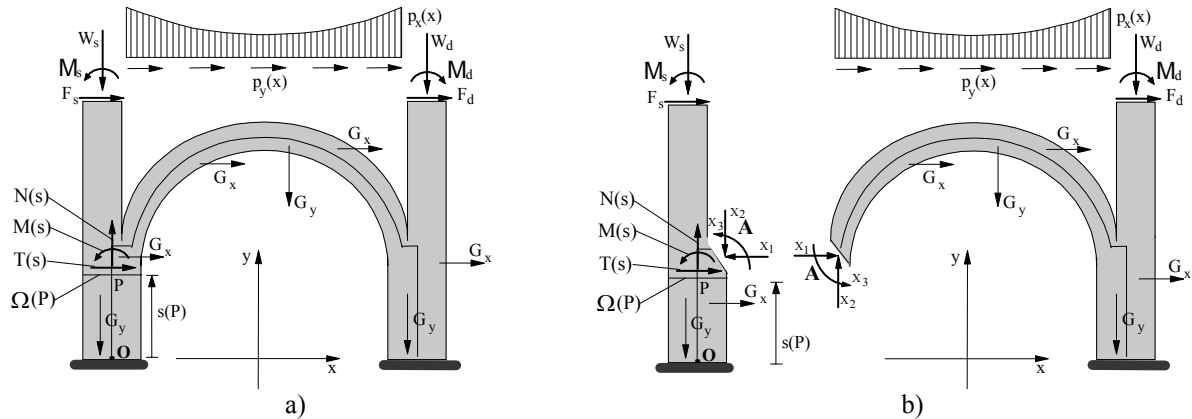


Figure 1. a) Stress pattern on cross sections; b) and c) schemes for managing equilibrium stress fields

The solution of the No-Tension (or NT) structural problem is approached by the Minimum principle of the Complementary Energy, and the procedure aims at identifying the redundant reactions allowing internal and external constraint compatibility.

Let \mathcal{D}_0 be the definition set of the admissible NT stress fields in equilibrium with the applied loads; the stress field σ_0 is found as the constrained minimum of the Complementary Energy functional $U(\sigma)$ under the condition that the stress field is in equilibrium with the applied loads and compressive everywhere

$$U(\sigma_0) = \min_{\sigma \in \mathcal{D}_0} U(\sigma) = U_0 \quad (2.1)$$

The admissibility of the stress field (Baratta & Corbi, 2003; 2005) is guaranteed by the condition that the force funicular line is everywhere in the interior of the arch profile (Fig. 2)

$$\begin{cases} N(s) \leq 0 \\ -h'(s) \leq \frac{M(s)}{N(s)} \leq h''(s) \end{cases} \quad \forall s \in (0, \ell) \quad (2.2)$$

$$e(s) = \frac{M(s)}{N(s)} \quad (2.3)$$

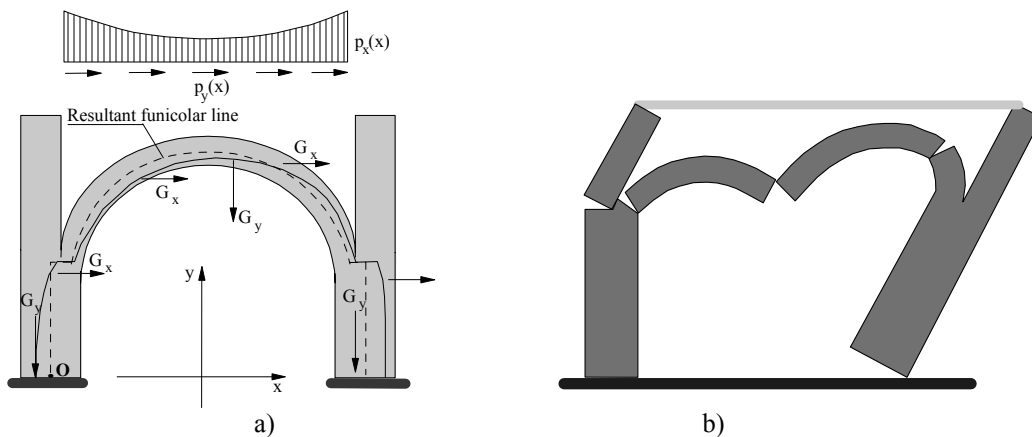


Figure 2. Admissible funicular line (a) and collapse for the theoretic model (b).

3. TESTS OF MASONRY ARCHES ON THE SHAKING TABLE

Near the Laboratory of the ENEA Research Center some tests on some simulacra are performed. The testing structure is represented by an arch built in tufa bricks rests on two piers, which continue over the impostes in order to contain the overload imposed on the top of the arch with the help of a tie-rod. The structure has a circular round-headed axis and the geometry shown in Fig. 3.

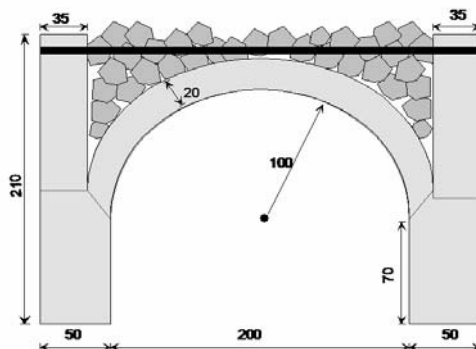


Figure 3. Specimen (in cm) of the masonry arch for the laboratory tests.

3.1. The tested structure: the masonry arch

The structure is made by local yellow tufa bricks tied by a poor mortar, which is a most common masonry encountered in South Italy. The intrados profile of the arcade is semicircular with a radius of 100 cm. The arcade is composed by two rows of bricks determining a masonry thickness of 20 cm; the two pillars which support the arcade have a rectangular base 50 cm and an height 70 cm; the depth of the whole is 100 cm. The wing walls, continuing in height the pillars, which have to contain the overload, are characterized by thickness 35 cm and an height 110 cm.

Moreover, some steel tie-beams fixed by means of flexible elastic ties are placed between the structure and the wing walls used for containing the overload, in order to guarantee the stability during the tests. The total weight of the masonry structure is 5,1 tons. On the top of the portal arch an overload of material composed by crushed tufa and lime and having a weight of 1,4 ton is applied, in order to simulate the structural context where the real arcade is included. Sliding is prevented through steel profiles attached to the shaking table.

The total weight of the structure plus the overload and the steel bars is 7,0 tons.

3.2. The soliciting and recording instruments

During the tests the seismic input is transmitted to the structure by means of a shaking table having: dimension of 4 x 4m, maximum supported weight of 10 ton, six degrees of freedom, frequency range of 0-50Hz, maximum peak acceleration of 3g, maximum velocity of 5m/sec and maximum span of 25cm.

In order to evaluate the time histories of the acceleration and displacement some recording instruments are located at some supposed "critical" positions on the arch, for the determination of the structure' response.

The recording instruments consist of two different typologies of accelerometers: 20 piezoelectric accelerometers with feed-through band of 2-15000 Hz ($\pm 10\%$), and nominal sensitivity of 10 pC/g, 8 transducers of displacement (LVDT) – which are subdivided in some transducers with nominal sensitivity of 0,1 Vmm-1 ($\pm 3\%$), maximum displacement of ± 2 inch, and feed-through band of 50 Hz, and other transducers with nominal sensitivity of 0,2 V/mm ($\pm 3\%$), maximum displacement of ± 1 inch, and feed-through band of 50Hz. The accelerometers are directly applied on the masonry arch, while the transducers are located in correspondence of the external sides of the two piers, and are fixed to some steel trestles integral with the shaking table.

3.3. The laboratory tests

At first the tuning of the shaking table is performed in order to check the response of the table and realize the test profile (1997; Clemente et al., 1999). Then the arches are tested.

The first arch having an overload on the top of the arcade fixed to 14,1 kN is tested in two phases up to the collapse. In the first phase (*Phase A*) an excitation corresponding to the time history recorded in Sturmo during the earthquake occurred in Campania-Lucania on the 23rd November 1980 with direction W-E, and increasing

amplitude from 0,3g up to 1,5g is used as horizontal input. Thereafter, in order to approach the collapse condition of the structure, in the second phase (*Phase B*), an increasing vertical input with amplitude of 1,5g is added to the horizontal input up to the collapse condition encountered at 1,8g. In both the two phases the applied excitation acts in the plane of the structure, orthogonally to its side at the bottom of the portal arch. The first cycle of laboratory tests was stopped at the peak acceleration 1.5g and caused some damages on the structure never leading to its collapse. This unexpected result may be due to two major reasons: the first is because for any increment of the damaging a reduction of the own frequencies of the total apparent modes of the structure occurs, and the second reason is due to a-priori filtering applied on the lower-frequencies of the Sturmo accelerogram (Fig. 4).

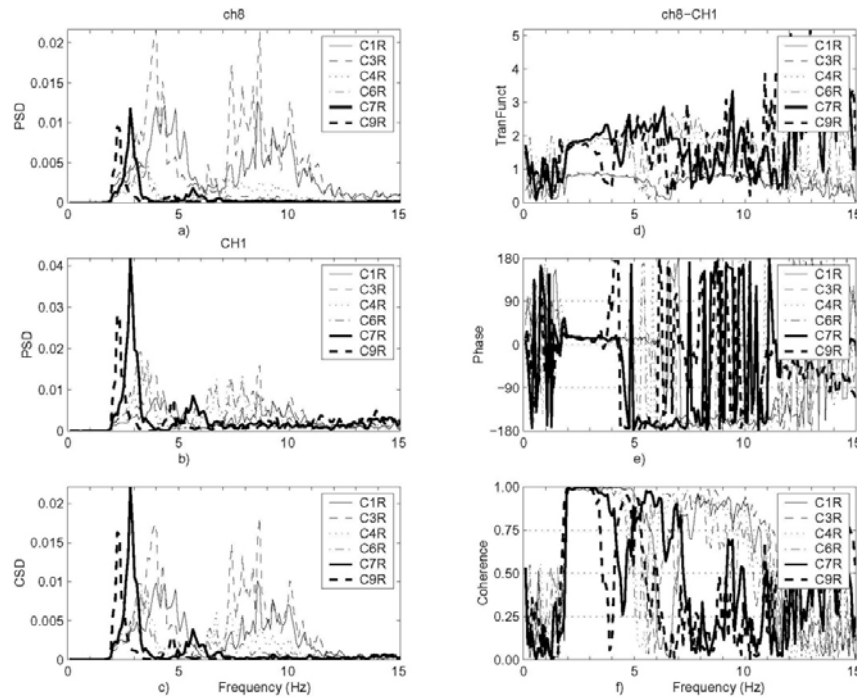


Figure 4. Sample of the recorded diagrams in the laboratory tests for different parameters.

Table 3.1. Laboratory tests on the second arch pre-consolidation.

TEST	SOLICITATION	NOTE
C1	white noise	Overload 8.5 kN. Tests start (cycle 1)
PI	pink noise_01	
C2	T1	test 01
	white noise	
P2	pink noise_02	
	T2	
C3	white noise	Overload 14.1 kN. New start of tests (cycle 2)
PIA	pink noise_01	
T1A	test 01	
C2A	white noise	
P2A	pink noise_02	
T2A	test 02	
C3A	white noise	Test stop for breaking off of some stones
P3A	pink noise_03	
C1R	white noise	Restoration of the broken bricks and new start of the test (cycle 3)
T1R	test 01	
C2R	white noise	
T2R	test 02	
C3R	white noise	
T3R	test 03	
C4R	white noise	
T4R	test 04	
C5R	white noise	
T5R	test 05	
C6R	white noise	
T6R	test 06	
C7R	white noise	
T7R	test 07	Test stop for breaking off of some stones.
C8R	white noise	Characterization following to the previous test
C8RB	white noise	Characterization before the testing start
C8RATT	white noise	Characterization with a scale spectrum 1/2
T7RB	test 07	Final test
C9R	white noise	

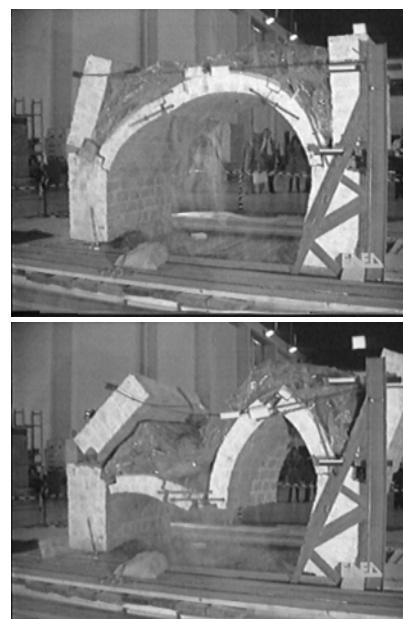


Figure 5. Tests of the second arch till the collapse.

On the second arch a sequence of seismic tests with increasing intensity is transmitted, by assuming as base signal the W-E component of the acceleration time history recorded at Sturno during the earthquake of Campania-Lucania (Italy) on the 23rd November 1980; moreover, a varying overload on the top of the arcade is introduced. In Table 1 the tests on the second are detailed. The base acceleration is always applied into the longitudinal direction, determining a plane stress state, unless of spatial effects due to the presence of unavoidable executive defects. Three cycles of tests with different overload and excitation are developed in order to study the behavior of the second arch: cycle 1, with an overload of 8,5kN applied on the top of the portal arch, and a seismic input consistent of a white noise for the seismic characterization of the structure, a pink noise and two tests of 0,1 and 0,2g; cycle 2, with an overload of 14,1kN (equivalent to the one acting on the first arch) and two seismic tests performed with peak 0,1 and 0,2g (the cycle is then interrupted because of the detachment of some stones at the intrados), cycle 3, started after the restoration of the broken bricks, an overload of 14,1kN is kept, the pink noise which is probably the cause of the masonry slack is removed, and the seismic tests are continued up to the peak acceleration of 0,7g (Fig. 5).

4. COMPARISON BETWEEN EXPERIMENTAL TESTS AND THEORETICAL MODEL

4.1. The elaboration of the laboratory tests' data

By plotting the data recorded during the laboratory tests on a diagram of the frequencies f (Hz) with respect to the seismic intensity (the coefficient " $c = a_p/g$ ") some evidences between the two arches are shown (Fig. 6). Both the arches show a typical behavior where the trend of the recorded frequencies decreases with respect to the seismic intensity the arch has been subjected, approximately according to an exponential curve. Nevertheless the dynamic curve of the first arch decreases more quickly than the curve of the second arch. Probably this effect is due to the different program of the shaking sequences to which the arches have been subjected during the tests: in the tests of the second arch an increasing pink noise has been coupled to the Sturno input, with the result to anticipate the damage of the arch.

This different behavior is pointed out in Fig. 6 where the decay of the first own frequencies of the two arches is shown. The fact is however that the trend of both curves can be approximated by an exponential curve, the curve relevant to the first arch decreases more quickly than the second one.

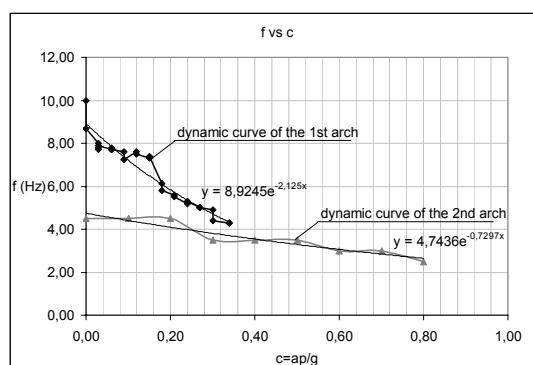


Figure 6. Comparison between Recorded data (black points) and the dynamic curves (exponential trend lines) of the structural frequencies f (Hz) vs the seismic coefficient $c = a_p/g$ during the laboratory tests on the two arches.

In the estimate of the seismic vulnerability of a existing masonry structure under a seismic input, at first the static analysis yielding the fundamental elements of the examined masonry structure can be solved by considering only the geometric dimensions and some other easily collectable data. So the trend of some characteristic displacement parameter u_c (e.g. the maximum displacements of points of the structure u_{max}) with respect to the seismic coefficient c can be inferred up to the collapse condition for $c = c_f$ (Fig. 7a). The derivative of the seismic coefficient c gets the trend of the tangential stiffness $K = K(c) = c'(u)$ as a function of the displacement u_{max} and of the coefficient c (Fig. 7b).

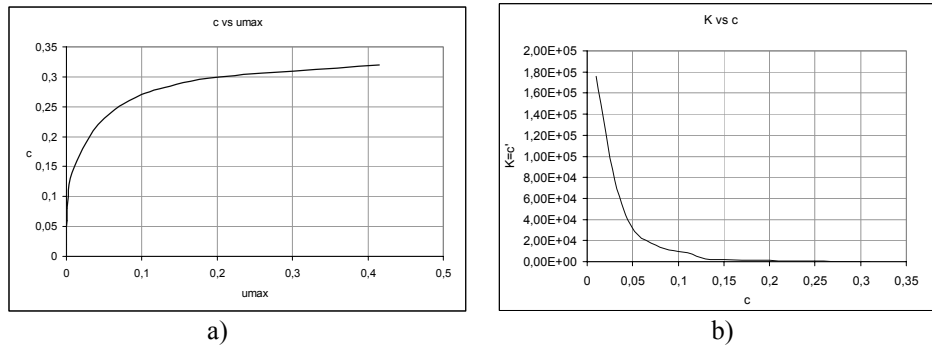


Figure 7. a) Trend of the seismic coefficient c vs the maximum displacements u_{max} by the static calculus; b) trend of the tangential stiffness $K=c'(u)$ vs the seismic coefficient c (b) by the static calculus.

Two verisimilar assumptions can be made. The first assumption consists on that the own frequency of the structure is a function of the type $f_0^2 = \alpha^2 K_0$, where K_0 is the stiffness of the structure. Since the structure has a NT non-linear behavior (Fig. 7a), the frequency is expected to depend on the stress intensity, that is measured by c , so the frequency can be supposed as expressed by $f^2(c) = \alpha^2 K(c)$, being $K(c)$ the tangential stiffness.

After dynamic characterization on the structure in site (e.g. by soliciting the fabric with a white noise or other) the own frequency f_0 is identified before any earthquake strikes on the building. This allows to estimate the coefficient $\alpha = f_0 / \sqrt{K_0}$, after calculating the initial stiffness K_0 . It is found that, heuristically, the curve $f(c) = \alpha \sqrt{K(c)}$ follows an exponential proceeding (Fig. 8a). This curve is referred to in the following as the “static damage progression”.

Moreover, a second sentence can be assumed, i.e. that also the progression of damage in a sequence of earthquakes with increasing intensity is of the exponential type, as observed in the experiments that have been summarized in the above. This curve is referred to in the following as the “dynamic damage progression”.

So the static and the dynamic curves, $f^*(c)$ and $f(c)$ respectively, can be directly compared, after having been reported to the same initial frequency $f(0) = f^*(0)$ (Fig. 8 a-b).

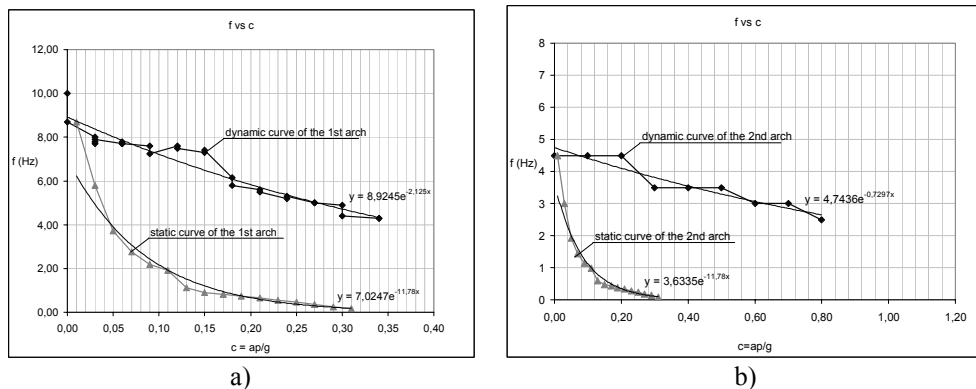


Figure 8. Comparison between the trend of the frequency f vs the seismic coefficient c by the static calculus (triangles) and by the seismic tests (squares), and the relevant exponential approximations, for the first masonry arch (a) and for the second masonry arch (b).

Consider that damage and consequent proneness to seismic collapse evolves according to an exponential law, e.g. having the form assumed in the following

$$f(c) = f_0 e^{-qc} \quad (4.1)$$

where c is the intensity of the worst earthquake the structure has suffered in the past and to which it has survived. At the same time the own frequency f_0 , i.e. the easiest parameter that can be evaluated by dynamic identification, evolves with increasing the damage of the structure.

So, if one looks at the derivative of the expression and its ratio in Eq. (4.1), one gets

$$f'(c) = -f_0 q e^{-qc} = -q f(c) \quad \rightarrow \quad \frac{f'(c)}{f(c)} = -q \quad (4.2)$$

The rate of decay of the own pulsation turns out to be constant, despite the fact that in a nonlinear structure it is to be expected that the hazard increases with the intensity of the ground shaking.

4.2. The comparison between the static and dynamic results

Moreover some basic observations can be made about the experimental data. The first is that the seismic decay of the own frequency of the arch when increasing the seismic intensity can be modeled by means of an exponential curve. Then, the static degradation of the arch, inferred by means of the static calculus on an NT arch, can be approximated by an exponential curve as well (Fig. 7b). The degradation is here measured by the variations of the tangential stiffness with respect to the increasing of the seismic component of the overload.

By the comparison of the exponential approximations of the static and dynamic curves, shown in Figs. 8a and 8b, it is evident that the static degradation appears to be much faster than the dynamic one. This effect is probably caused by the opening of the fractures in the arch that produces an increasing absorption of the oscillation energy as kinetic energy at the limit for the mechanism activation, rather than as elastic energy. It is possible to emphasize some tentative approach that is possible to draw on the basis of the experimental results.

By the observation of the diagrams, it can be considered that the two exponential curves (“static” and “dynamic” curves) can assume a very similar form by changing the scale of the abscissas c . So, considering that the static curve obeys the equation

$$f^* = f_0^* e^{-q^* c} \quad (4.4)$$

while the dynamic curve obeys Eq. (4.1), it is clear that if the “static” c is multiplied times q^*/q , the two curves become very similar. If the same transformation is applied to the ordinates in the static calculus line (Fig. 7b), one obtains a very significant increase in the seismic capacity of the structure, approximately a seismic peak acceleration that is 5 times larger than the limit static force.

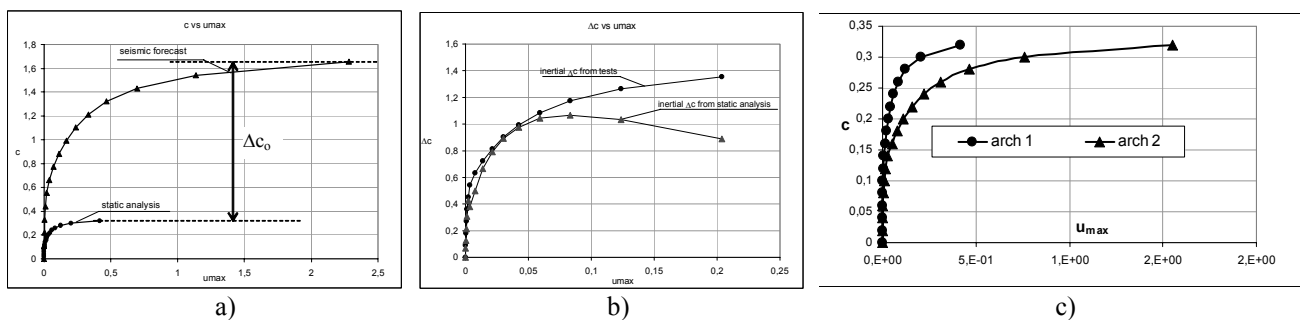


Figure 9. a) Final pseudo-force/displacement curve under seismic action; b) experimental absorption of inertia forces in accordance with Eq. (4.6); c) comparative seismic forecasts for both arches.

This result would agree with test, so that it has been necessary to rise the peak ground acceleration up to 1.8g to bring the arch to collapse. It is necessary to remark that the difference between the “seismic” and the “static” curve is due to inertial forces due to accelerations involved in the arch deformation.

Such accelerations a can be grossly related to the maximum displacements u_{\max} through the pulsation ω_0 by a relation of the type

$$a = \omega_0^2 u_{\max} \quad (4.5)$$

It should be expected that the difference Δc between the two curves in Fig. 9 can be referred to some additional displacements Δu_{\max} that, according to Eq. (4.5), is given by

$$\Delta c = \frac{\Delta a}{g} = \frac{\omega_0^2 \Delta u_{\max}}{g} \quad ; \quad \Delta u_{\max} = \frac{g \Delta c}{\omega_0^2} \quad (4.6)$$

where $\Delta a = g \Delta c$.

This is a necessary condition for additional inertial forces absorption. In Fig. 9b the experimental values of Δc are plotted versus u_{\max} as expressed in Eq. (4.6).

By adding the additional displacement to the abscissas in Fig. 9a, one gets a possible reconstruction of the relationship between the peak acceleration and the maximum displacement under seismic excitation

The procedure can be applied to both arches, yielding comparative results of the seismic forecast as in Fig. 9c.

CONCLUSIONS

By comparing the dynamic curves of the tested arches (Fig. 6), which can be well approximated to an exponential form, one observes that the curve relevant to the first arch decreases more quickly than the second one. Moreover, by the comparison of the exponential approximations of the static and dynamic curves (Fig. 8a), it is evident that the static degradation is much faster than the dynamic one. This effect is probably caused by the opening of the fractures in the arch that produces an increasing absorption of the oscillation energy as kinetic energy, mainly due to the progressive activation of a collapse mechanism, rather than as elastic energy. The considerations illustrated in Sec. 4.3 enable a transformation of the static analysis results to produce a "seismic response expectation" as in Fig. 9b. Looking at the results of the static analysis elaborated to yield seismic expectation (Fig. 9c) the second arch has to produce larger displacements than the first one, to store a given amount of elastic energy. This means that a larger part of the external energy displayed by the earthquake has to be transformed by the second arch in kinetic energy through the activation of a mechanism. The larger the amplitude of such mechanism the faster the arch approaches collapse.

ACKNOWLEDGEMENTS

The laboratory tests were funded by the ENEA Research Center (New technology Department, Rome, Italy) and by the Authority of the Monumental Heritage Supervision in Benevento and Caserta Provinces. The recent advancements have been performed thanks to the financial support by the Department of Civil Protection of the Italian Government, through the RELUIS Pool (Convention n. 540 signed 07/11/2005, Research Line n. 8).

REFERENCES

- Baratta, A. (1995) The no-tension approach for structural analysis of masonry buildings. Proc. of the Fourth International Masonry Conference, British Masonry Society, London.
- Baratta A., Corbi I. Corbi O., D. Rinaldis D. (2008). Experimental Survey on Seismic Response of Masonry Models. Proc. of 6th International Conference on Structural Analysis of Historical Construction SACH 2008, 2-4/7/2008, Bath, UK.
- Baratta, A. & Corbi O. (2003). The No Tension Model for the Analysis of Masonry-Like Structures Strengthened by Fiber Reinforced Polymers. *Intern. Journal of Masonry International, British Masonry Society*, **16: 3**, 89-98.
- Bintrim, J.W., Laman, J.A. & Boothby, T.E. (1998). Dynamic testing of masonry arch bridges. In Sinopoli A. (ed.) Arch bridges, Proc. Second International arch Bridge Conference held in Venice: 295-303, Rotterdam, Balkem.
- Brown G., Pretlove A.J., Ellick, J.C.A., Hogg, V. & Choo, B.S. (1995). Changes in the dynamic characteristics of a masonry arch bridge subjected to monotonic loading to failure. In Melbourne C. (ed.) Arch bridges, proc. First International Arch Bridge Conference held in Bolton, London: 375-383.
- Clemente, P., Buffarini, G., Rinaldis, D. & Baratta, A. (1999). Changes in the dynamic characteristics of a masonry arch subjected to seismic actions. Proc. of the Fourth European Conference on Structural Dynamics, EURO DYN'99, Prague, Czech Republic.